Available online at www.sciencedirect.com

ScienceDirect

Journal of the European Ceramic Society 31 (2011) 421–427

www.elsevier.com/locate/jeurceramsoc

Technical note

ZrO_2 removing reactions of Groups IV–VI transition metal carbides in ZrB_2 based composites

Ji Zou[a,b], Guo-Jun Zhang[a,*], Shi-Kuan Sun[a,b], Hai-Tao Liu[a,b], Yan-Mei Kan[a],
Ji-Xuan Liu[a], Chang-Ming Xu[a]

[a] *State Key Laboratory of High Performance Ceramics and Superfine Microstructures, Shanghai Institute of Ceramics, Shanghai 200050, China*
[b] *Graduate School of the Chinese Academy of Sciences, Beijing 100049, China*

Received 5 July 2010; received in revised form 3 October 2010; accepted 6 October 2010
Available online 30 October 2010

Abstract

In this paper, ZrO_2 removing reactions of Groups IV–VI transition metal carbides (MCs, M = Hf, Nb, Ta, W, Ti and V) in ZrB_2 based ultra-high temperature ceramics (UHTCs) are investigated. Distinct roles of various MCs were observed during this process. According to thermodynamic analysis and experiment verifications, the sequence for oxide removing ability of different MCs is WC > VC > NbC > TaC > HfC > TiC. The importance of this study concerns the establishment of a map of reactivity of the transition metal carbides against ZrO_2, in order to choose the proper additive for the densification of ZrB_2-composites.Utilizing right reactions and controlling proper sintering atmospheres, high density ZrB_2–SiC ceramic could be eventually obtained by pressureless sintering at temperatures (around 2000–2200 °C).

Keywords: ZrB_2; Chemical reactions; Transition metal carbide (MC); Oxygen contamination; Pressureless sintering (PLS)

1. Introduction

Studies on ZrB_2–SiC based ultra-high temperature ceramic (UHTCs) have primarily dealt with aerospace applications; a typical example is the sharp leading edges for maneuverable hypersonic flight vehicles and re-usable atmospheric re-entry vehicles.[1] The densification issues of ZrB_2 based composites have been overcome through different sintering technologies in recent years,[2–4] however, the realization of the full potential applications of UHTCs still needs the efforts to improve the thermo-mechanical properties[5] and oxidation[6,7]-ablation[8] resistance.

Composition design is one of the important methods to improve these performances of UHTCs.[1,4,7] In recent years, much effort has been devoted to seek proper third phases to improve both the densification process and the properties of ZrB_2–SiC.[1] Among these additives, Groups IV–VI transition metal carbides (MC) are of great interest in relation to the multiple effects they induce once added to ZrB_2-composites. The effects of MCs could be classified into several categories and summarized as follows:

(i) Previous studies have demonstrated that the addition of MC (e.g. WC[9] and VC[10]) can accelerate the densification of ZrB_2–SiC.
(ii) MCs can improve the mechanical properties of ZrB_2–SiC. ZrB_2–SiC–WC composites with bending strength over 1 GPa have been reported.[11] The high strength has been argued to result from a small grain size of ZrB_2 and the presence of WC. In another independent work, WC was found to be helpful for the formation of elongated ZrB_2 grains, and high toughness ZrB_2–SiC composites were obtained by pressureless sintering below 2200 °C.[12] Furthermore, Wu et al. reported that the in situ formed ZrC substantially improved the sintering behavior and fracture toughness of ZrB_2–SiC–ZrC ceramics.[13,14]
(iii) The addition of certain kinds of MC can enhance the ablation resistance of ZrB_2–SiC.[15] The ablation measurement of the sample with compositions ZrB_2–20 vol% ZrC–16 vol% SiC showed that its conversion depth and

---

[*] Corresponding author. Tel.: +86 21 52411080; fax: +86 21 52413122.
E-mail address: gjzhang@mail.sic.ac.cn (G.-J. Zhang).

0955-2219/$ – see front matter © 2010 Elsevier Ltd. All rights reserved.
doi:10.1016/j.jeurceramsoc.2010.10.011

Table 1
Characteristics of the raw materials.

Material	Particle size (D_{50})	Impurities (%)	Supplier
ZrB_2	14 μm	O 0.5, Na 0.01, Al 0.01, Ca 0.06, Fe 0.2, Si 0.01, Hf 1.5, Ti 1.9, V 0.01	Gongyi Sanxing Ceramics Materials Co., Ltd.
Milled ZrB_2	1.4 μm	O 1.7, others were not analyzed	Same as above
α-SiC	0.45 μm	B 0.33, O 1, Ca 0.24, Cl 0.1, Fe 0.16, V 0.09	Changle Xinyuan Carborundum Co., Ltd.
WC	<1 μm	NA[b]	Hard alloy Co., Ltd., Zhuzhou, China
MC[a]	1–3 μm	NA[b]	Beijing Mountain Technical Development Center Beijing, China
ZrO_2	0.3 μm	NA[b]	CSG Holding Co., Ltd., Shenzhen, China

[a] M = Ti, V, Hf, Nb and Ta.
[b] Not analyzed.

conversion rate were superior to that of ZrB_2–20 vol% SiC under active condition with a heat flux of 400 W/cm^2 and a pressure of 0.042 atm.[15]

The chemical reactions of MC in ZrB_2–SiC are investigated in order to better understand their roles in the system and obtain the desirable properties of ZrB_2–SiC–MC.

As we know, ZrO_2 and B_2O_3 are always present on the surface of ZrB_2 particles. Most B_2O_3 could be removed by heating in vacuum during the sintering process, while the removing of ZrO_2 is difficult.[9,16,17] The complexity of the chemical reactions in ZrB_2–SiC–MC systems increases due to surfacial zirconia impurities. Till now, two kinds of reactions have been reported in ZrB_2–WC[9] and ZrB_2–VC systems.[10,18] One reaction path (Type I) is that MC reduces ZrO_2 (Reaction (1)) and evolves the gas of CO.

$$ZrO_2 + 3MC \rightarrow ZrC + 3M + 2CO\uparrow \quad (1)$$

The other path (Type II) is the high temperature interchange reaction between MC and ZrB_2 (Reaction (2)).

$$ZrB_2 + MC \rightarrow ZrC + MB_2 \quad (2)$$

Apart from WC and VC, there are a number of transition metal carbides with high melting points, a systematic study of the effect of their addition on the sintering behavior of ZrB_2–SiC and the related chemical reaction mechanisms constitutes an interesting issue. The purpose of this paper is to investigate one kind of high temperature reactions of MC in ZrB_2–SiC systems (Type I), and the primary applications of these reactions are also assessed. The transition metal carbides considered in the present work are WC, VC, TaC, TiC, NbC and HfC. All of them belong to Groups IV–VI.

2. Experimental procedures

Commercially available ZrB_2, ZrO_2, various transition metal carbides and SiC powders were used as raw materials. Their particle sizes and suppliers are listed in Table 1. In order to reduce their grain sizes, ZrB_2 powder was previously planetary milled for 8 h in acetone before used.

2.1. Powder processing, sample preparation and sintering

(1) ZrO_2–MC

Powder mixtures of ZrO_2 and MC (mole ratio is set as 1:3) were ball milled in ethanol for 24 h, and then dried and ground into powders. About 5 g of each mixed powder was uniaxially pressed into pellets with a diameter of 12 mm. Sintering was carried out in a graphite element furnace in vacuum, and the final sintering temperatures were set at 1650, 1900 and 2100 °C, respectively. After soaked at the highest temperature for 1 h, pellets were cooled down to room temperature naturally.

(2) ZrB_2–SiC (ZS)–MC

80 vol% ZrB_2–20 vol% SiC with external 5 vol% MC (based on the total volume of ZrB_2 and SiC) powder mixtures (ZS–MC) were suspended in acetone and ball milled for 12 h. After drying the slurry through a rotary evaporator at 70 °C, the powder mixture was crushed, and screened (−200 mesh). In pressureless sintering experiments, the as-treated powder mixture was cold compacted with dimensions of 37 mm × 30 mm × 5 mm under a pressure of 250 MPa, and sintered at temperatures between 2000 and 2200 °C. The detailed sintering program is similar to our previous work.[12]

2.2. Sample characterization

After removing the surface layer of the sintered samples by grinding, XRD was used to determine the phase assemblage as well as the chemical reactions in different samples. The relative density of some sintered specimens was measured using the Archimedes method. Some fracture surfaces of pellets were observed by scanning electron microscope (SEM).

3. Results and discussion

If the reactions between ZrO_2 and MC are favorable before the occurrence of ZrB_2 grain coarsening (1700–1800 °C), they can accelerate the densification of ZrB_2 powder compact by removing ZrO_2 from the ZrB_2 particle surface.[16] Till now, only two previous works have estimated the possibility to eliminate ZrO_2 by WC[9] or VC[18] by thermodynamic calculations. However, it should be noted that a series of non-stoichiometric

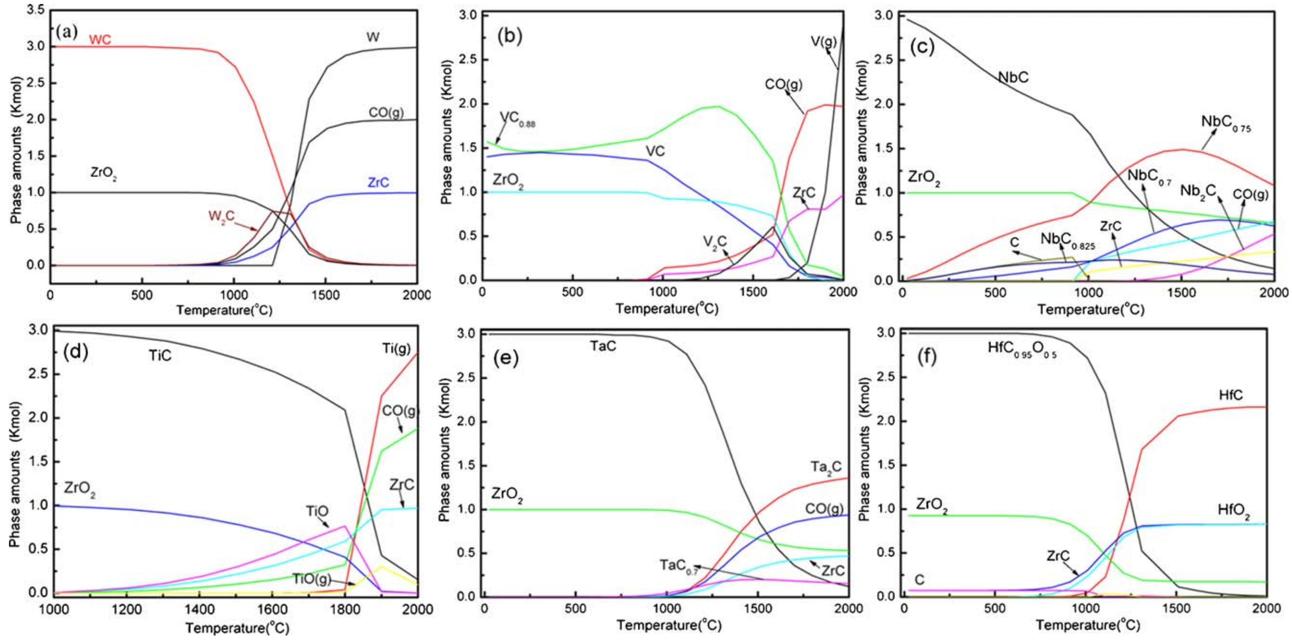

Fig. 1. Molar content of the products calculated by reactions between 3 mole MC and 1 mole ZrO_2 as a function of the temperature at a vacuum level of 5 Pa. (a) WC, (b) VC, (c) NbC, (d) TiC,(e) TaC, and (f) HfC.

transition metal carbides, such as W_2C, $Nb_{0.7}C$, $TaC_{0.7}$, could exist in the present systems. Hence, the discussions centering only on the change of Gibbs free energy as a function of temperature for certain reaction may not be full-scale. To solve this problem, an equilibrium composition mode based on a commercial software (HSC Chemistry for Windows 6.1, Outokumpu Research Oy, Pori, Finland) was used throughout the thermodynamic considerations (Fig. 1).

3.1. Thermodynamic considerations

Reaction (1) is strongly affected by the partial pressure of CO (g), and a reduction of the CO partial pressure causes an increased driving force for the removal of ZrO_2 by MC. So the total equilibrium pressure in these systems must be considered in the thermodynamic analysis. It is set as 5 Pa, which is the approximately the vacuum level maintained in the furnace during the soaking period in the sintering process.

Thermodynamic predictions show that ZrO_2 could react with MC at certain temperature. However, the reaction process and the resultant products are different varying the transition metal carbide.

(1) WC and VC (Fig. 1(a) and (b)). A feature found during the vacuum heating in these systems is the existence of an intermediate phase M_2C (e.g. W_2C and V_2C), formed after the dissociation of MC (Reaction (3)).

$$MC = MC_x + (1 - x)C(0 < x < 1) \tag{3}$$

Most of the ZrO_2 can be removed below 1650 °C by the successive reactions with the as-formed C (Reaction (4)) or M_2C (Reaction (5)).

$$2C + ZrO_2 = ZrC + 3CO \quad (g) \tag{4}$$

$$3M_2C + ZrO_2 = 6M + ZrC + 2CO \quad (g) \tag{5}$$

ZrC and the corresponding transition metal elements (tungsten (W) and vanadium (V)) are the final reaction products. Different from W, the melting point of V is about 1900 °C, so a large amount of gaseous V would be drawn out of the furnace above 2000 °C. The evidence for the existence of vanadium vapor is that some silvery white residuals (contain V) were always found on the surface of the graphite paper after sintering ZrB_2–SiC–VC.[10]

(2) NbC and TaC (Fig. 1(c) and (d)). Similar to WC, non-stoichiometric carbides also appeared in this system. Thermodynamic predictions indicate that the formation of NbC_x and TaC_x by Reaction (3) becomes favorable above 1000 °C. Partial ZrO_2 could react with C (derived from the decomposition of NbC and TaC). However, the subsequent reactions between residual ZrO_2 and newly formed NbC_x (or TaC_x) are extremely difficult. ZrO_2, as a main phase, still exists as one of the equilibrium components when the temperature reached 2000 °C upon thermodynamic calculation.

(3) TiC and HfC (Fig. 1(e) and (f)). An exchange reaction between carbide and ZrO_2 (Reaction (6)), rather than the ZrO_2 removing reactions (Reaction (1)), is more likely in this system at mild temperatures according to thermodynamic analysis.

$$MC + ZrO_2 = ZrC + MO \quad \text{or} \quad MO_2$$
$$(M = Hf \quad \text{and} \quad Ti) \tag{6}$$

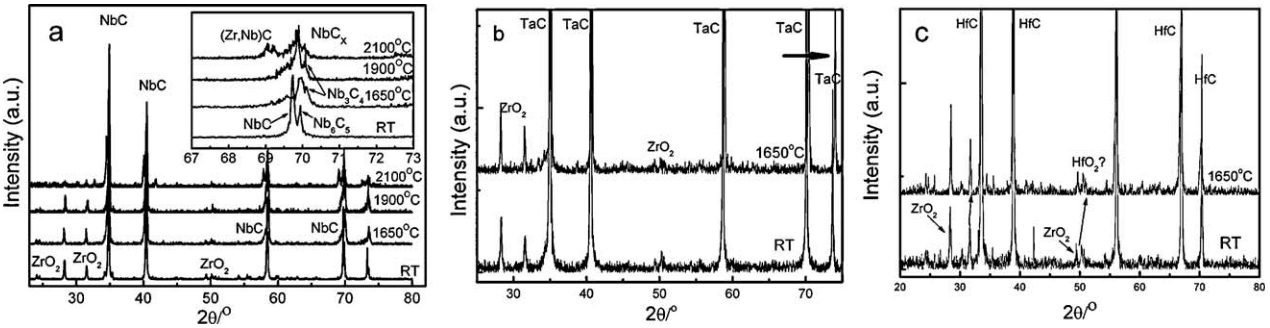

Fig. 2. XRD patterns of NbC–ZrO_2 (a), TaC–ZrO_2 (b), HfC–ZrO_2 (c) pellets sintered at different temperatures for 1 h in vacuum.

Though ZrO_2 could be removed during this process, other oxides (e.g. HfO_2 and TiO) still remain in the products based on thermodynamic calculations. What's more, when the temperature is higher than 1800 °C, Reaction (2) becomes thermodynamically favorable in ZrO_2–TiC system, and the latter case is very similar to that in the ZrO_2–VC system mentioned above.

3.2. Experimental verification of the oxide removing reactions by MC

Two recent studies[9,10,14] have reported the reactions processes between ZrO_2 and VC or WC, and the results are in partial accordance with the above thermodynamic considerations, the differences between experiment and thermodynamic calculation have also been compared. In ZrO_2–WC systems,[9] traces of W_2C still remained in the samples after sintering at 2100 °C, which meant some kinetic factors restricted the complete reaction in ZrO_2–W_2C. On the other hand, in ZrO_2–VC systems,[18] an intermediate phase (VC_xO_y) was experimentally observed, but not expected by the thermodynamic calculation due to the lack of thermodynamic data in the current commercial software.

To experimentally verify the reactions which have not been proved, pellets containing ZrO_2 and some representative transition metal carbides MC (here, M = Nb, Ta, Hf) were sintered at different temperatures in vacuum. Their corresponding XRD patterns are shown in Fig. 2.

In accordance with the thermodynamic calculations, the peaks for ZrO_2 still appeared in ZrO_2–NbC mixtures even after heat treatment at 1900 °C for 1 h (Fig. 2(a)). Furthermore, NbC_x was observed when the temperature increased, and normally the x value was decreased with the increase of temperature (i.e. 0.875 at 1650 °C and 0.75 at 1900 °C). This means that the "release" of carbon from NbC occurred in this temperature range. The new formed carbon could further react with a small amount of ZrO_2 to become ZrC (see the inset image of Fig. 2(a)) or (Zr,Nb)C solid solutions.

In ZrO_2–TaC mixtures, though no separate peaks belonging to TaC_x were observed in Fig. 2(b), all the peaks for TaC showed a shift to a higher 2θ value compared to their original positions after sintering at 1650 °C. This cannot be explained by the incorporation of Zr atom in TaC. If Zr would substitute Ta into the TaC lattice, the bigger covalent radius of Zr (1.59 A) compared to Ta (1.43 A)[19] would have enlarged the average unit-cell size of TaC, and shifted the diffraction peak to a lower 2θ value. In fact, the lattice parameter (a) of TaC_x decreased with reducing x value,[20] $a(x) = 4.3007 + 0.1563x$. So the peak shift should be attributed to the formation of a non-stoichiometric TaC_x. The removal of ZrO_2 by TaC was also essentially achieved by the reaction of C and ZrO_2. Because the release of C from TaC was very sluggish, the effective role of TaC on removing ZrO_2 was restricted. The above analysis strongly supports the thermodynamic viewpoint.

In the third case of ZrO_2–HfC mixture, only a slight peak change was observed before and after the samples was sintered (Fig. 2(c)). It is hard to identify whether an exchange reaction (Reaction (6)) existed in this system, since the peak positions of ZrO_2 and HfO_2 are very close and they can form a solid solution with each other. However, Reactions (1) and (3) did not occur in this system as calculated in Fig. 1(f).

According to the remaining amount of oxides (ZrO_2 plus MO, MO_2, and other solid state oxides) predicted by thermodynamics, the oxide removing ability of different carbides could be compared (Table 2). The sequence is as follows, WC > VC > NbC > TaC > HfC > TiC. Transition metal carbides of Group VI have the best oxide removing ability, followed by those of Group V. The carbides in Group IV preferred to react with ZrO_2 by an exchange reaction (Reaction (6)) rather than the oxide removing reaction (Reaction (1)), and a possible reason might be their similar crystal structures and outer electrons distributions in the same group. The results (Table 2) also show that Cr_3C_2 is another kind of additives which can react with ZrO_2 effectively, and a positive effect on the densification of ZrB_2 could be expected.

Table 2
Residual oxide amounts (ZrO_2 plus MO, MO_2, and other oxides) predicted by thermodynamics at different temperatures. ZrO_2 is set as 1 mole and MC is set as 3 mole.

	WC–ZrO_2	VC–ZrO_2	NbC–ZrO_2	TaC–ZrO_2	HfC–ZrO_2	TiC–ZrO_2	Cr_3C_2–ZrO_2
1300 °C	0.31	0.89	0.81	0.97	0.99	1.03	0.00
1700 °C	0.01	0.3	0.71	0.88	0.99	1.17	0.00

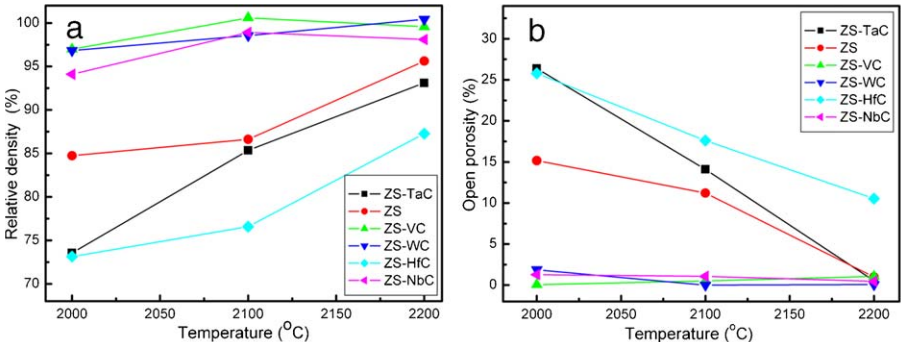

Fig. 3. Relative density and open porosity of ZS ceramics with and without transition metal carbides sintered at different temperatures.

On the other hand, based on the above discussions, the stability sequence of ZrO_2–MC ceramics at high temperatures (1300–1700 °C) in vacuum could be compared.

The sequence is $WC–ZrO_2 < VC–ZrO_2 < NbC–ZrO_2 < TaC–ZrO_2 < HfC–ZrO_2 < TiC–ZrO_2$. As we know, ZrO_2–MC nanoceramics exhibited very excellent mechanical properties (e.g. high bending strength (1–1.5 GPa) and fracture toughness (5–7 MPa m$^{1/2}$)[21,22]), and attentions should be paid to their applications in vacuum at high temperature atmospheres (above 1300 °C). A direct application of such oxide removing reactions has been shown in the following sections.

3.3. Applications: pressureless densification of ZrB_2–SiC by different MCs addition

It is well known that additives which can react and promote the removal of ZrO_2 below 1700 °C can accelerate the densification of ZrB_2. Some transition metal carbides can remove ZrO_2; in this section, the effect of some carbides, namely WC, VC, HfC, NbC and TaC, on the densification of ZrB_2–SiC (ZS) composites were analyzed.

The relative density and open porosity along with the sintering temperatures were measured for ZrB_2–SiC composites with or without transition metal carbides additions (Fig. 3). Generally speaking, the use of MC as sintering aid significantly changed the densification curve of ZS. The relative density of ZS increased obviously with the elevated sintering temperature, reaching 85% TD at 2000 °C. However, a continuous increase of the relative density for ZS related to a systematic increase of the sintering temperature was not observed. It was still below 96% TD even if the sintering was conducted at 2200 °C for 2 h.

A noticeable change of the final density was observed when MC was added. WC or VC containing specimen demonstrated an increased density, and full densified samples could be obtained at as low as 2000 °C; nevertheless, the addition of TaC and HfC seems to deteriorate the same process. The relative densities of ZS–TaC and ZS–HfC were even lower compared with ZS in the same temperature range. The changes in open porosity (Fig. 3(b)) indicate that most of the pores in all the specimens are open below 2100 °C, and the trends of decreasing open porosity are in accordance with the increase in relative density as shown in Fig. 3(a). The density results are consistent with the prediction by oxide removing ability of the MCs shown in Section 3.2.

The driving force of the sintering could be increased by the ratio of the grain boundary energy (γ_{GB}) of as-sintered ceramics and the surface energy (γ_{SV}) of raw particles. A clean particle surface without oxide contamination can increase the γ_{SV} of the corresponding powder. So the reasons for the fact that carbides affected the densification of ZrB_2–SiC could be explained by the different abilities to remove oxides (ZrO_2) from ZrB_2 particle surfaces, which is in agreement with that discussed in Section 3.2.

The fracture surfaces of ZS with and without carbide additions are shown in Fig. 4. Considering that the average grain sizes of initial ZrB_2 was 0.45 μm, a remarkable grain growth occurred in VC, NbC or WC doped samples after held at 2100 °C, about 10 μm (primarily observed by SEM), while only the neck formation accompanied by isolated pores was found in ZS, ZS–TaC, ZS–HfC. It has been demonstrated that without removing surface oxygen contamination, grain coarsening in boride particles could be promoted through an evaporation-condensation process by surface diffusion at intermediate temperatures,[23] while their densifications by the grain boundary diffusion was restricted. Neck formation with unchanged distance between the contacting grains is the characteristics of such mechanisms (Fig. 4(f)).

Based on the two-particle model, the change of neck radius (x, as described in Reaction (7)) is associated with saturated vapor pressure (P_0), surface energy (γ) of the particles and sintering time (t) (Reaction (7)) when evaporation-condensation mechanism dominates.[24] The saturated vapor pressure of ZrB_2 and ZrO_2 is relatively low (below 10^{-4} Pa at 2000 °C), so the matter transport process between ZrB_2 particles was extremely slow, and the densification of ZS, ZS–TaC and ZS–HfC was very difficult.

$$x^3 = C_{\text{eveporation}} P_0 \gamma t \tag{7}$$

When the oxide contamination on the surface of ZrB_2 particles was removed by VC or WC, the densification induced by a grain boundary diffusion occurred (Fig. 4). The change of neck radius was connected with self-diffusion coefficient (D^*), surface energy of the particles (γ) and sintering time (t) (Reaction (8)).[24]

$$x^5 = C_1 D^* \gamma^2 t \tag{8}$$

where coefficient $C_{\text{evaporation}}$ and C_1 depend on the materials and temperature.

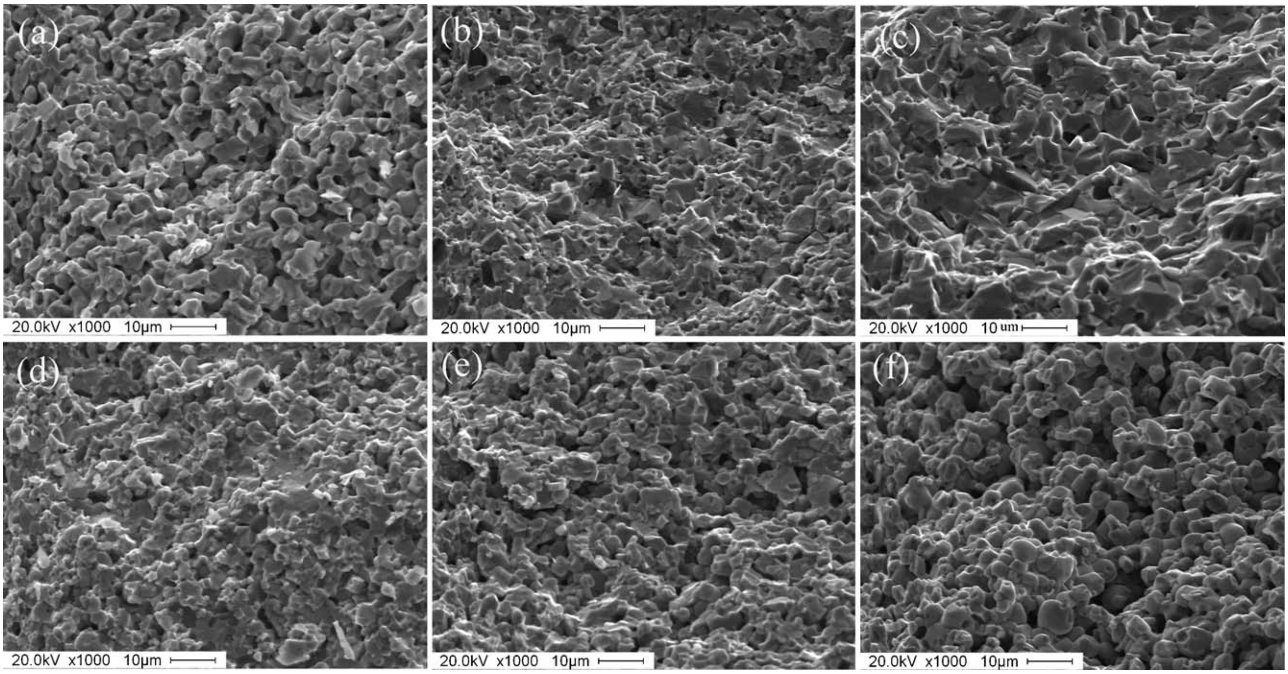

Fig. 4. Fracture surface of the samples sintered at 2100 °C. (a) ZS; (b) ZS–WC; (c) ZS–VC; (d) ZS–NbC; (e) ZS–TaC; (f) ZS–HfC.

Though the lack of data for the self-diffusion coefficient of ZrB_2, D^* of HfB_2 has been reported to be 7×10^{-11} cm^2/s from 1700 to 1900 °C, which is comparable to that of conventional ceramic (e.g. MgO and Al_2O_3) at the same temperature range,[25] and a similar D^* value range of ZrB_2 could be estimated. Once the dominant sintering mechanism was changed to grain boundary diffusion, the densification process (ZS–VC and ZS–WC) remarkably accelerated as shown in Fig. 3(a).

The reasons for the harmful effect of some carbide additions (such as HfC) on the densification process of ZrB_2–SiC during pressureless sintering will be discussed. First, monolithic HfC ceramic is hard to be sintered due to its strong covalent bonds,[26,27] and a series of previous works reported that extremely high temperatures (2200–2690 °C)[26] are needed for densification even by hot pressing. This temperature is obviously higher than that of ZrB_2 based composites. Second, the additions of HfC particles restricted ZrB_2 grains growth, which in return, inhibited the densification of the composites. Third, at such high sintering temperature (2100–2200 °C), the oxide removing reactions (Reaction (1)) between ZrO_2 and HfC may occur, and the gaseous CO may not be completely released from the partially densified sample. Once the gaseous components remained incorporated in the samples, they become pores which are difficult to eliminate during the following sintering stages.

4. Conclusions and perspectives

The process of oxide removal in transition metal carbides (MC) doped ZrB_2–SiC composites, and the high temperature reactions between ZrO_2 and MC were investigated. All of the MC belonging to Groups IV–VI could react with ZrO_2. However, the oxide removing ability, reaction process and the products are quite different. The effective mechanisms for the oxide removing process by MC could be described as: (1) The decomposition of MC to MC_x and C; (2) The reaction between C and ZrO_2; (3) The reaction between MC_x and the remaining ZrO_2. The former two steps could be observed in most of the MC (except HfC and TiC) at mild temperatures, while the realization of the last step could only be realized in VC and WC systems, which made them good additives for pressureless sintering of ZrB_2 based composites. The oxide removing ability is a good rule to evaluate the effectiveness of the sintering aids for pressureless sintering of ZrB_2 based ceramics when choosing transition metal carbides as sintering additives (e.g. Cr_3C_2 in Table 2).

Acknowledgements

Financial support from the Chinese Academy of Sciences under the Program for Recruiting Outstanding Overseas Chinese (Hundred Talents Program), the National Natural Science Foundation of China (No. 50632070), International Science and Technology Cooperation Project of Shanghai (No. 08520707800) and the CAS Special Grant for Postgraduate Research, Innovation and Practice are greatly appreciated.

References

1. Fahrenholtz WG, Hilmas GE, Talmy IG, Zaykoski JA. Refractory diborides of zirconium and hafnium. *J Am Ceram Soc* 2007;**90**:1347–64.
2. Sciti D, Silvestroni L, Nygren M. Spark plasma sintering of Zr-and Hf-borides with decreasing amounts of $MoSi_2$ as sintering aid. *J Eur Ceram Soc* 2008;**28**:1287–96.
3. Brochu M, Gauntt BD, Boyer L, Loehman RE. Pressureless reactive sintering of ZrB_2 ceramic. *J Eur Ceram Soc* 2009;**29**:1493–9.
4. Hu CF, Sakka Y, Tanaka H, Nishimura T, Guo SQ, Grasso S. Microstructure and properties of ZrB_2–SiC composites prepared by spark plasma sintering using $TaSi_2$ as sintering additive. *J Eur Ceram Soc*; in press.

5. Monteverde F, Scatteia L. Resistance to thermal shock and to oxidation of metal diborides–SiC ceramics for aerospace application. *J Am Ceram Soc* 2007;**90**:1130–8.
6. Talmy IG, Zaykoski JA, Opeka MM. High-temperature chemistry and oxidation of ZrB_2 ceramics containing SiC, Si_3N_4, Ta_5Si_3, and $TaSi_2$. *J Am Ceram Soc* 2008;**91**:2250–7.
7. Wu HT, Zhang WG. Fabrication and properties of ZrB_2–SiC–BN machinable ceramics. *J Eur Ceram Soc* 2010;**30**:1035–42.
8. Monteverde F, Savino R, De Stefano Fumo M, Di Maso A. Plasma wind tunnel testing of ultra-high temperature ZrB_2–SiC composites under hypersonic re-entry conditions. *J Eur Ceram Soc* 2010;**30**:2313–21.
9. Zhang SC, Hilmas GE, Fahrenholtz WG. Pressureless densification of zirconium diboride with boron carbide additions. *J Am Ceram Soc* 2006;**89**:1544–50.
10. Zou J, Zhang GJ, Kan YM, Wang PL. Pressureless densification of ZrB_2–SiC composites with vanadium carbide. *Scripta Mater* 2008; **59**:309–12.
11. Chamberlain AL, Fahrenholtz WG, Hilmas GE, Ellerby DT. High-strength zirconium diboride-based ceramics. *J Am Ceram Soc* 2004;**87**:1170–2.
12. Zou J, Zhang GJ, Kan YM. Formation of tough interlocking microstructure in ZrB_2–SiC-based ultrahigh-temperature ceramics by pressureless sintering. *J Mater Res* 2009;**24**:2428–34.
13. Wu WW, Zhang GJ, Kan YM, Wang PL. Reactive hot pressing of ZrB_2–SiC–ZrC composites at 1600 °C. *J Am Ceram Soc* 2008;**91**:2501–8.
14. Wu WW, Zhang GJ, Kan YM, Wang PL. Reactive hot pressing of ZrB_2–SiC–ZrC ultra high-temperature ceramics at 1800 °C. *J Am Ceram Soc* 2006;**89**:2967–9.
15. Bull J, White MJ, Kaufman L. Ablation resistant zirconium and hafnium ceramics. United States Patent 5,750,450; 12 May 1998.
16. Fahrenholtz WG, Hilmas GE, Zhang SC, Zhu S. Pressureless sintering of zirconium diboride: particle size and additive effects. *J Am Ceram Soc* 2008;**91**:1398–404.
17. Zhang SC, Hilmas GE, Fahrenholtz WG. Pressureless sintering of ZrB_2–SiC ceramics. *J Am Ceram Soc* 2008;**91**:26–32.
18. Zou J, Zhang GJ, Kan YM, Wang PL. Hot-pressed ZrB_2–SiC ceramics with VC addition: chemical reactions, microstructures, and mechanical properties. *J Am Ceram Soc* 2009;**92**:2838–46.
19. Post B, Glase FW, Moskowitz D. Transition metal borides. *Acta Metall* 1954;**2**:20–5.
20. Hackett K, Verhoef S, Cutler RA, Shetty DK. Phase constitution and mechanical properties of carbides in the Ta–C system. *J Am Ceram Soc* 2009;**92**:2404–7.
21. Malek O, Lauwers B, Perez Y, De Baets P, Vleugels J. Processing of ultrafine ZrO_2 toughened WC composites. *J Euro Ceram Soc* 2009;**29**:3371–8.
22. Anne G, Put S, Vanmeensel K, Jiang DT, Vleugels J, Van der Biest O. Hard, tough and strong ZrO_2–WC composites from nanosized powders. *J Euro Ceram Soc* 2005;**25**:55–63.
23. Baik S, Becher PF. Effect of oxygen contamination on densification of TiB_2. *J Am Ceram Soc* 1987;**70**:527–30.
24. Kang SJL. *Sintering: densification, grain growth and microstructure*. Oxford: Elsevier Butterworth-Heinemann; 2005.
25. Kalish D, Clougherty E. Densification mechanisms in high-pressure hot-pressing of HfB_2. *J Am Ceram Soc* 1969;**52**:26–9.
26. Courtright EL, Prater JT, Holcomb GR, Stpierre GR, Rapp RA. Oxidation of hafnium carbide and hafnium carbide with additions of tantalum and praseodymium. *Oxid Met* 1991;**36**:423–37.
27. Liu JX, Kan YM, Zhang GJ. Synthesis of ultra-fine hafnium carbide powder and its pressureless sintering. *J Am Ceram Soc* 2010;**93**:980–6.